ISSN 0102-7468

CBPF-MO-004/87

DISCRETE VARIATIONAL METHODS AND THEIR APPLICATION TO ELECTRONIC STRUCTURES

by

D.E. Ellis[1] and D. Guenzburger[1,2]

[1]Centro Brasileiro de Pesquisas Físicas - CNPq/CBPF
Rua Dr. Xavier Sigaud, 150
22290 - Rio de Janeiro, RJ - Brasil

[2]Northwestern University, Evanston, IL, U.S.A.

CONTENTS

1. INTRODUCTION

The Discrete Variational (DV) approach to the solution of integro-differential equations utilizes a basis set and sampling techniques which can be adapted to a wide variety of physical problems. Self-consistent field models of nuclear and electronic structure lead to *single particle* problems, such as the familiar Schrödinger equation

$$(h-\varepsilon_i)\,\psi_i(\vec{r}) = 0 \qquad (1)$$

in which a number of states ψ_i, i=1,2,...N are coupled together in a nonlinear fashion through the effective potential of the Hamiltonian h. In this context, both Hartree-Fock and Local Density (LD) theories have been extensively applied[1-5].

The sampling approach becomes more and more interesting as the number of degrees of freedom (dimensionality) of the physical system increases. The *many particle* problem of electronic structure provides opportunities for application of error-minimization strategies in the $(\vec{r}_1,\vec{r}_2)$ space of six dimensions. The matrix secular equations of Configuration Interaction (CI) theory and the sums of one- and two-body interaction integrals of Many-Body Perturbation Theory (MBPT) can be reformulated as integro-differential equations, of the general form[6,7]

$$\mathcal{L}_1 \quad (\phi_i^a) = 0 \;;\; \mathcal{L}_2(\phi_{ij}^{ab}) = 0 \;;\ldots \qquad (2)$$

Here $\mathcal{L}_i$ contain kinetic energy, external potential, and electron-electron interaction operators, and ϕ_i^a, ϕ_{ij}^{ab},... are a set of res-

ponse functions corresponding to selected classes of single particle ($i \to a$), two-body ($ij \to ab$), and higher excitations from some reference state characterized by a set of orbitals $\{i\}$. The resulting inhomogeneous equations (2) provide a little explored alternative to the tedious integral summations of conventional methods. Also, the structure of the functions $\phi_i^a, \phi_{ij}^{ab}, \ldots$ can provide much insight into the nature of important electronic correlation processes in atomic and molecular systems.

Classical problems of *structural and fluid mechanics* are also well suited to the DV scheme, whether formulated as path integrals

$$\delta \int_1^2 \mathcal{L}(\rho, \vec{r}, t)\, ds = 0 \tag{3}$$

or as partial differential equations in canonical coordinates[8] $\{q_i\}$,

$$\frac{\partial \mathcal{L}}{\partial q_i} - \frac{d}{dt} \frac{\partial \mathcal{L}}{\partial \dot{q}_i} = 0 \tag{4}$$

In the following sections we will develop general concepts and a way of thinking about approximation which will hopefully enable the students at this school to design and implement DV methods optimal for their particular research interests. Examples will be presented for electronic spectra, charge densities, and bonding of free molecules, surface-chemisorbed species, and bulk solids.

2. GENERAL CONCEPTS

Functions of a continuous variable may be represented by a *discrete set* of function values:

$$\psi(\vec{r}) \sim \{\psi(\vec{r}_i)\} \quad i=1,2,\ldots N \tag{5}$$

and *basis functions* provide an interpolation onto the continuous field, e.g.,

$$\psi(\vec{r}) \simeq \sum_i \psi(\vec{r}_i)\, \chi_i(\vec{r}). \tag{6}$$

Here generalized Lagrange polynomials satisfying $\chi_i(\vec{r}_j)=\delta_{ij}$ reproduce function values on the given grid, and $\{\chi_i\}$ can further be chosen to satisfy boundary conditions and smoothness criteria.

It is useful to draw a distinction between *global expansions* and *local fits*; suppose

$$\psi(\vec{r}) \simeq \sum_i C_i \chi_i(\vec{r}). \tag{7}$$

Then in a global expansion the coefficients $\{C_i\}$ are defined over the entire domain of interest $\vec{r} \in \Omega$ as in, for example the familiar LCAO (linear combination of atomic orbitals) representation of molecular wave functions. In a local fitting scheme Ω is divided into subdomains Ω_λ, with coefficients $\{C_i^\lambda\}$ and functions $\{\chi_i^\lambda\}$ defined for $\vec{r} \in \Omega_\lambda$. The multiple scattering (MS) or Green's function representation of wavefunctions provides an example of this type[9].

Global expansions have the advantage of generating simple equations for solution of the given integro-differential equa-

tion. Conditions of continuity and differentiability are trivially satisfied by choice of χ_i, as are asymptotic boundary conditions. The price paid for this convenience is use of a rather large basis, and consequently solution of a rather large set of linear equations in a typical application. Conversely, local fits can provide a very compact and efficient representation; however, the additional work required to satisfy matching conditions at subdomain boundaries can be considerable.

There are a number of related techniques of approximation which can be mentioned at this point. The traditional method of *discretization* of differential equations provided the first foundation for approximate solutions. Here operators like $\frac{\partial}{\partial X}$ are approximated by finite differences; e.g.

$$\frac{\partial f(x,y)}{\partial X} \simeq \frac{f(x+\Delta,y)-f(x,y)}{\Delta} \tag{8}$$

and a selected grid of points (x_i,y_j), $\begin{matrix} i=1,2,\ldots N \\ j=1,2,\ldots M \end{matrix}$ leads to a coupled set of equations in $f(x_i,y_i)$ of order NM. For one- and two-dimensional problems this finite difference approach is reasonably effective[10]. If the desired solution ψ has much structure dense grids are required, and as the number of dimensions increases this approach rapidly becomes intractable.

The *finite element* methods which today dominate the fields of structural mechanics, diffusion, fluid flow and related two - and three-dimensional problems, represent a more sophisticated approach to grid and basis selection. Here the function is represented by local fits; e.g.

$$f(\vec{r}) \simeq \sum_i C_i^\lambda \, g_i^\lambda(\vec{r}) \qquad \vec{r} \in \Omega_\lambda \tag{9}$$

over nonoverlapping polyhedra Ω_λ. The interpolating functions g_i^λ are typically polynomials of low order, centered on each of the nodes $\vec{r}_i^\lambda$ of the grid which is formed from the vertices of the polyhedra. Function values $f(\vec{r}_i^\lambda)$ and possibly their derivatives $\vec{\nabla} f(\vec{r}_i^\lambda)$ provide variational parameters which are coupled both by the target differential equation, and by boundary conditions between adjacent subdomains[11].

A large fraction of the effort involved in finite element calculations involves choice of a node set optimal for a particular problem. Since the amount of computation involved per point is considerably greater than in simple finite difference schemes, it is important to develop *nonuniform* grids, which are sparse in regions where f is smoothly varying, and dense in regions where f has considerable structure. Nested grids, with small polyhedra fitting inside larger ones, are frequently used for this purpose; e.g., tetrahedra in 3 dimensions (3D).

The final class of methods we will discuss deal with averages or *moments* of various properties taken over the sample grid. An *error moment* approach is particularly closely related to discrete variational schemes used in molecular and solid state problems. Suppose we want to satisfy $\mathcal{L} f = 0$; then define $\mathcal{L} f(\vec{r}) = E(\vec{r})$ and call E the "local error". A strategy for producing an E which is in some sense a minimum will constitute an approximate solution. Define a sample average as

$$\langle g \rangle = \sum_i w_i g(\vec{r}_i) \tag{10}$$

and then satisfy

$$\langle \phi_j E \rangle = 0 \qquad j=1,2,\ldots M \tag{11}$$

with functions $\{\phi_j\}$ and weight $w_i = w(\vec{r}_i)$ suitably chosen.

As an example, consider a mean square error minimization, with an expansion of the type given in Eq. (7). Then

$$\langle |E|^2 \rangle = \sum_i w_i \left(\sum_j \mathcal{L}\chi_j C_j\right)^* \left(\sum_k \mathcal{L}\chi_k C_k\right) \tag{12}$$

and the conditions $\frac{\partial \langle |E|^2 \rangle}{\partial C_j} = 0$ $j=1,2,\ldots M$ give a homogeneous set of linear equations for $\{C_j\}$. However, if $\mathcal{L} = h-\varepsilon$, the equations are quadratic in the eigenvalue ε.

Linear methods which converge to the conventional Rayleigh-Ritz variational integral approach provide our final, and most practical example. Let $\{\phi_i\} = \{\chi_i^*\}$ and require

$$\langle \chi_i^* \sum_j \mathcal{L}\chi_j C_j \rangle = 0 \qquad j=1,2,\ldots M \tag{13}$$

This gives a Hermitean matrix;

$$\mathcal{L}_{ij} = \sum_p w_p \chi_i^*(\vec{r}_p) \mathcal{L}\chi_j(\vec{r}_p) \tag{14}$$

and with $\{w_p, \vec{r}_p\}$ corresponding to an integration rule one recovers the standard Rayleigh-Ritz equations[3,4]. In particular, for the Schrödinger equation,

$$(\underset{\approx}{H} - E \underset{\approx}{S}) \underset{\approx}{C} = 0 \tag{15}$$

3. PRACTICAL ASPECTS

A. Sampling Schemes

By now it is clear that the choice of a sampling scheme is one of the more important issues in constructing an efficient DV method. If no prior information is used, *unbiased random* sampling is always available, with sample means converging as $N^{-1/2}$, where N is the number of points. *Pseudorandom* sampling such as the diophantine scheme developed by Haselgrove can produce results which converge as N^{-k}, where k depends upon the smoothness (differentiability) of the integrand[12]. Here we are considering sampling as a method of approximate integration; however, we note that the convegence of eigenvalues and wavefunction coefficients is roughly equivalent. The *prefactor* E_o controlling the error in a given property, $E \sim E_o N^{-k}$ is controlled by other factors involving detailed and deliberate error cancellation.

Potential singularities at nuclear sites in the SCF electronic Hamiltonian (and r_{12}^{-1} in the CI case) limit the convergence rate to k=1. However, *weighted pseudorandom* sampling is effective in reducing E_o greatly. The general idea can be simply illustrated: suppose we want to calculate the integral $\int f(x)dx$. Then a change of variable gives $\int (f \frac{dx}{dy}) dy$, and if we are able to map $x \leftrightarrow y$ such that $dy/dx = f^{-1}$, then a single point will produce the *exact* result! Of course, such one to one mappings are never available in cases of interest. It is perfectly feasible to generate distributions of sample points with density $D(\vec{r})$ roughly similar to the integrand, and $w \sim D^{-1}(\vec{r})$ provides a suitable weight function. In a typical DV application, there are hundreds or thousands of matrix elements, so it is pointless to optimize sampling for a single case. A pseudo-

random grid consisting of a few hundred points per atom ($\sim 10^3$ for heavy elements) with a distribution function consisting of a sum of radial Fermi-functions centered on the nuclei is sufficient for most spectroscopic studies, at the LD single particle level of theory.

In principle, one can obtain highly accurate results with a very small number of points. The *pseudospectral* methods of Friesner[13] and others require of the order of one point per variational coefficient. Such highly optimized sampling leads to difficulties associated with the so-called "aliasing problem", which are also encountered with periodic sampling. Nevertheless, one has the perspective of developing a stable algorithm with an order of magnitude fewer points than present-day technology.

Conventional integration schemes of the Gauss-polynomial type[14] are hopelessly inefficient for the full 3D or 6D space of a molecule. However, we have found that a mixed scheme, consisting of a regular integration mesh covering a spherical region around each nucleus, and a pseudorandom sample in the interstitial and exterior regions, provides good *wavefunction* accuracy in both core and valence regions. Such a scheme, with a modest increase in sampling effort compared to simple pseudorandom, is well suited for calculation of hyperfine properties[15]. Finally, we want to mention the adaptation of classical integration methods by Baerends et al.[16] to very accurate integration rules for molecular structures.

B. POTENTIAL APPROXIMATIONS

The lectures of Prof. Pedroza[17] and workshop discussions have focussed on the approximations of LD theory which lead to various forms of effective exchange and correlation potential V_{xc}. Our purpose here is to consider some little discussed but critical aspects of approximate solution of the Poisson equation $\nabla^2 V_c = -4\pi\rho$ (16) to obtain the Coulomb potential. In fact, so-called "shape-approximations" to solutions of Eq. (16) are often responsible for differences (i.e., errors) in eigenvalues and other properties which are greater than those attributable to V_{xc} approximations.

The *muffin-tin* potential is of considerable interest, since it is central to the use of multiple scattering wavefunctions. Here V_c is approximated by a spherical average in spherical regions around each nucleus, a *constant* in interstitial regions, and spherical in exterior regions:

$$V_{MT}(\vec{r}) = V_\lambda(r_\lambda) \qquad r \in \Omega_\lambda \tag{17}$$

$$= V_o \qquad r \in \text{interstitial}$$

The Schrödinger and Dirac equations can be solved exactly in this model potential, using a partial wave (angular momentum) representation.

The potential truncation implied by Eq. (17) is reasonably small for close-packed metallic systems; it becomes a major source of error for open structures such as semiconductors and free molecules. The MS wavefunctions can be used as a basis set, in such cases, for more accurate calculations with a refined potential. The

Linearized Muffin Tin Orbital (LTMO) scheme represents a highly successful application of this technique[18].

The Self-Consistent Charge (SCC) approximation to V_c has been used in a variety of DV molecular and solid studies; it is based upon approximating the charge density by a sum of spherical overlapping atomic distributions.

$$\rho \simeq \rho_{SCC} = \sum_{\nu n \ell} \rho^{\nu}_{n\ell} \left| R^{\nu}_{n\ell}(r_\nu) \right|^2 \qquad (18)$$

Here $\{R^{\nu}_{n\ell}\}$ are the radial wavefunctions used in the LCAO basis set and $\{\rho^{\nu}_{n\ell}\}$ are amplitudes determined either analytically as Mulliken orbital populations[19] or numerically as a least-squares fit to ρ on the sample grid[4,20]. The corresponding potential V_{SCC} is obtained by one-dimensional integration and summation. This potential has a range of utility somewhat larger than V_{MT}, is easy to generate, and uses parameters (populations) which have chemical intuitive appeal.

For highly accurate calculations and for situations where the concentration of charge in localized covalent bonds is important, the least-squares approach is capable of extension to the required precision. In the Self-Consistent Multipolar (SCM) approximation the expansion of Eq. (18) is extended as

$$\rho \simeq \rho_{SCM} = \sum_{\nu n \ell} \rho^{\nu}_{n\ell} \left| R^{\nu}_{n\ell}(r_\nu) \right|^2 + \sum_{\nu n L} g^{\nu}_{n\ell}(r_\nu)\, Y_L(\hat{r}_\nu) \ . \qquad (19)$$

Here $\{g^{\nu}_{n\ell}\}$ are radial functions centered on each nucleus, $L=(\ell,m)$ labels the spherical harmonics $\{Y_L\}$ also centered on nuclei.

Selection of the form of radial functions $\{g^{\nu}_{n\ell}\}$ is largely a matter of convenience; Slater-type expansions, Gaussians,

and highly localized polynomials have been used[4,16,20]. From the point of view of LD theory it is advantageous to generate model (fitted) densities, and to calculate potentials and related properties to high precision using the model densities. Graphical displays of fitting errors $\Delta\rho(\vec{r})$ are very helpful in identifying and removing systematic shortcomings.

C. SELECTION OF BASIS SETS

The methods which we have been describing are very flexible with respect to choice of basis functions; it is only necessary to be able to evaluate χ_j and $\mathcal{L}\chi_j$ numerically. This freedom permits one to select bases on grounds of boundary conditions, ease of calculation, and physically motivated interpretation. The use of analytic Slater-type orbitals (STO) of the form $r^{n-\ell-1}e^{-\rho r}y_L(\hat{r})$ and Cartesian Gaussian orbitals (GTO) $x^i y^j z^k e^{-\rho r^2}$ centered on nuclei (or off-center as well for GTO) is well developed in standard applications of HF, CI, and MBPT methods.

Accumulated experience in selecting and optimizing basis parameters can thus be exploited. The disadvantage of using analytic bases is that they do not satisfy the asymptotic properties of the exact wavefunctions; in consequence, the convergence rate of solutions with number of functions used can be slow. Since GTOs do not satisfy the cusp condition at the nucleus, their convergence is inferior to that of STOs. Neither type of function is capable, with a single term, of describing both valence- and long-range behavior of the single-particle HF or LD states of interest.

Numerical solutions of appropriate model Hamiltonians do

not suffer from these shortcomings. The functions

$$\phi_i^{\nu} = R_{n\ell}(r_{\nu}) Y_L(\hat{r}) \qquad (20)$$

are readily generated by standard atomic SCF codes. The radial wavefunctions are stored in tabular form, and values for arbitrary $\vec{r}$ are retrieved by polynomial interpolation. Since a free atom or negative ion has only a limited number of bound states, a procedure is needed to extend the basis. This is accomplished most simply by embedding the atom in a potential well, with parameters chosen to control the spatial extent of excited state orbitals[19].

When is a basis set sufficiently complete? What is the optimum strategy for generating a "good" basis with minimum effort? These important practical questions have to be attacked on the basis of experience; there are few useful general rules, but a lot of folk-lore. From the point of view of physical interpretation it is better to have a compact basis, with a near-minimal number of parameters. We have already mentioned SCC approximations to the potential which generate effective atomic configurations $\{\rho_{n\ell}^{\nu}\}$. Optimization of the basis functions of Eq. (20) using these configurations generally produces a near-minimal set of reasonable quality, and also leads to useful interpretations of bonding mechanisms and excitation processes.

Most simple schemes fail at one time or another; the SCC basis iteration just described is no exception. An alternative approach which requires only a little more effort, is to produce a spherical average of the molecular or crystallize potential about each site, and to use this potential with suitable boundary conditions in generating $\{\phi_i^{\nu}\}$. Site-optimized orbitals of this type have

been found effective in binding energy studies on transition metal clusters and chemisorption complexes[21].

Using the group-theoretic methods described by Prof. Vianna[22], we generate symmetry orbitals (SO)

$$\chi_i^j = \sum_{\nu m} \phi^{\nu}_{n\ell m} w^{\nu}_{\ell m j} \tag{21}$$

with coefficients $\{w^{\nu}_{\ell m j}\}$ corresponding to irreducible representations of the symmetry group of the molecule, solid, surface, or chain. The benefits of transforming the AO basis to an SO set consist not only in reducing the size of the secular matrices (Eq. 15), but through selection rules and descent in symmetry arguments one obtains an understanding of the origins and possible excitations of the eigenstates.

4. TRANSITION STATES AND TOTAL ENERGY

In general the single particle HF and LD eigenvalues do *not* correspond to physically observable energies (Koopmans "theorem" and empirical practice notwithstanding). However, it is possible to construct pseudoparticle Hamiltonians whose eigenvalues *do* correspond to binding and excitation total energy differences[5]. Here we will consider a simple example, application of the *transition state* scheme to LD theory, since it is of great practical utility.

Suppose the total energy is expanded in a Taylor series in the orbital occupation numbers

$$E(\vec{n}) = E(\vec{n}_o) + (\vec{n}-\vec{n}_o).\vec{\nabla}_n E\big|_o + O(\delta n^2) \tag{22}$$

about some reference state $\vec{n}_o$. But we know that $\partial E/\partial n_i = \varepsilon_i$, the single particle eigenvalues, so

$$E(\vec{n}) - E(\vec{n}_o) = \sum_i \delta n_i \varepsilon_i(\vec{n}_o) + O(\delta n^2) \quad . \tag{23}$$

We can do better than this; choose the mean-value Hamiltonian

$$h(\bar{n}) = \frac{h(\vec{n}_o) + h(\vec{n})}{2} \tag{24}$$

then[5]

$$E(\vec{n}) - E(\vec{n}_o) = \sum_i \delta n_i \varepsilon_i(\bar{n}) + O(\delta n^3) . \tag{25}$$

In practice, a precision of $\sim \pm 0.2$ eV is observed, with respect to direct calculation of total energy differences for binding and valence-state excitations in molecules. By comparison with experiment, *ionization potentials* are generally found with an accuracy of ± 0.5 eV or better, which is about the level of uncertainty in V_{xc}. These transitions correspond to $n_i \to n_i - 1$; the *electron affinities* $n_i \to n_i + 1$ should be given to a similar accuracy-however, diffuse anion final states are harder to describe. Multielectron excitations such as *shake-up* ionization $(n_i, n_j, n_k) \to (n_i - 1, n_j - 1, n_k + 1)$ have also been successfully modelled using the transition state scheme.

As an example of interest in inorganic chemistry, let us briefly consider the dodeca-carbonyls $M_4(CO)_{12}$ with M=Co,Rh,Ir. These compounds are thoroughly characterized in solution and as molecular crystals through IR, optical, X-ray, electrochemical, and other techniques[23]. Since the CO groups are easily substituted,

they play a role as catalysts, analogs for surface chemisorption and reactive intermediates.

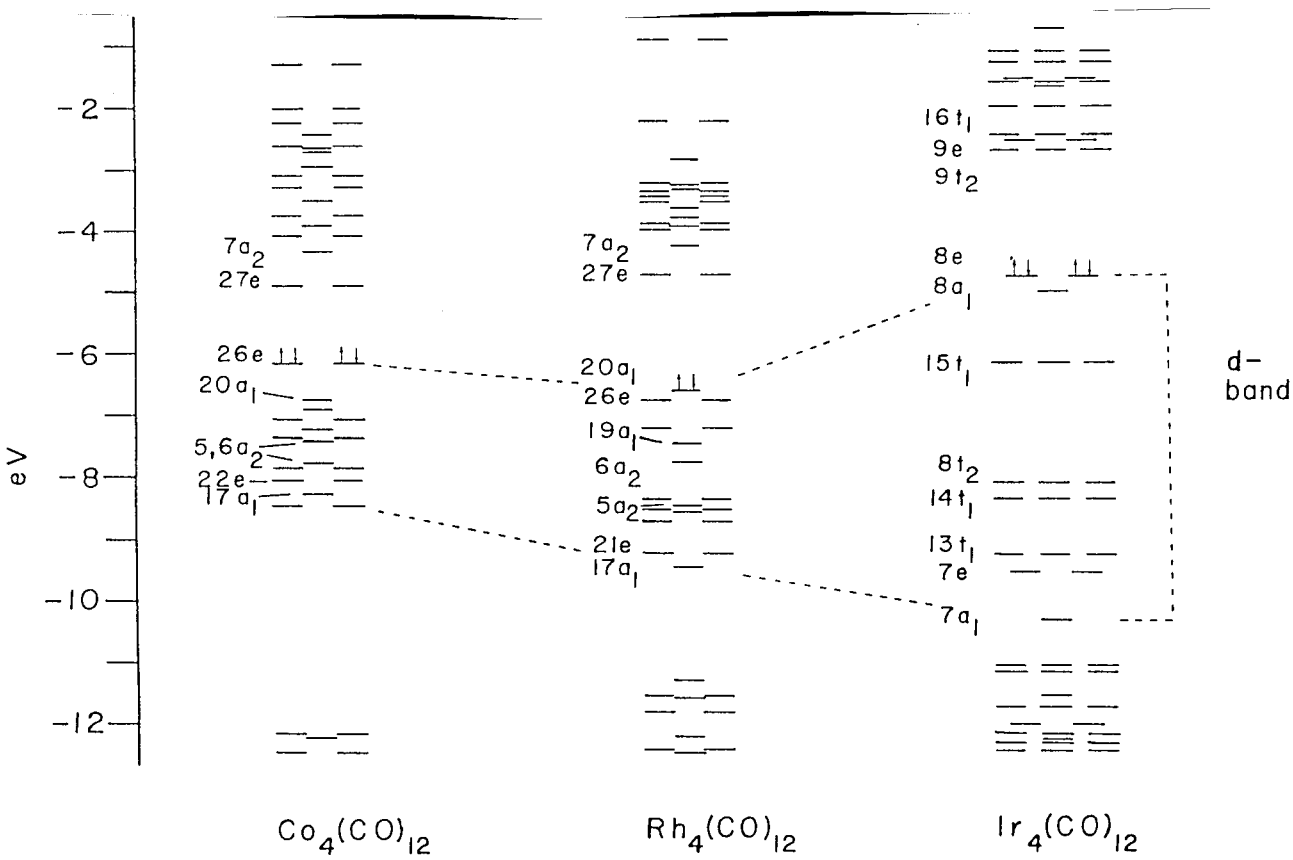

Fig. 1 - Ground state LD eigenvalues for $M_4(CO)_{12}$ free molecules (Ref.23); the highest occupied molecular orbital is indicated by a heavy line. For Co, the $26e \rightarrow 27e$ optical absorption edge and the $22e \rightarrow 27e$ intense $\sigma \rightarrow \sigma^*$ absorption are notable, and fit well with experiment.

The idea of *volume partitioning* of the total energy is very helpful in obtaining the bonding properties of fragments of molecules and solids. Let us write

$$E_{tot} = \sum_{\gamma} E_{\gamma} = \sum_{\gamma} \int_{\gamma} e(\vec{r})\, d^3r \qquad (26)$$

where γ denotes a nonoverlapping partitioning of the domain of interest, and e is the *local energy density*. In LD theory, as in HF, e consists of a single particle term, and two-body and exchange

corrections,

$$e(\vec{r}) = \rho_{\varepsilon}(\vec{r}) + W_{C}(\vec{r}) + W_{xc}(\vec{r}) . \tag{27}$$

The single particle part

$$\rho_{\varepsilon} = \sum_{i,\sigma} n_{i\sigma}\, \varepsilon_{i\sigma} \left| \psi_{i\sigma}(\vec{r}) \right|^{2} \tag{28}$$

the electron-electron, electron-nuclear and nuclear-nuclear Coulomb terms

$$W_{C} = -\frac{1}{2}\, V_{C}(\vec{r})\, (\rho_{nuc} + \sum_{\sigma} \rho_{\sigma}) , \tag{29}$$

and exchange-correlation corrections.

$$W_{xc} = \sum_{\sigma} \rho_{\sigma} (E_{xc,\sigma} - V_{xc,\sigma}) \tag{30}$$

are directly obtained as output of the SCF process. Here ρ_{nuc} is the (delta-function sum) nuclear charge distribution and ρ_{σ} represents the spin $\uparrow,\downarrow$ components of electronic density[20,24]. With volumes γ suitably chosen one can make a quantitative determination of the energy of an atom or of a specified bonding region. This volumetric approach provides an alternative to orbital-transformation schemes commonly used in fragment analysis, and is clearly independent of basis-set considerations.

5. EMBEDDED CLUSTERS

A. Models

A wide variety of embedded cluster schemes have evolved in response to the need to represent interaction of a cluster or molecular fragment with its environment. The most simple method is to place the cluster in a *potential field*, which in chosen to model the cluster-host interaction in an average sense. In HF and LD calculations it has been common to simply add a number of external point charges to model the electrostatic field of the host. In general we can write

$$h_{cluster} = h_{local} + V_{host} \tag{31}$$

with V_{host} generated by an array of point charges, distributed charge (e.g., uniform density, sheets of charge, spherical shells), distributed ions of finite radial extent, or in self-consistent LD form with

$$\rho(\vec{r}) = \rho_{cluster} + \sum_{\nu}^{host} \rho_{\nu} \tag{32}$$

An iteration schematic of the form

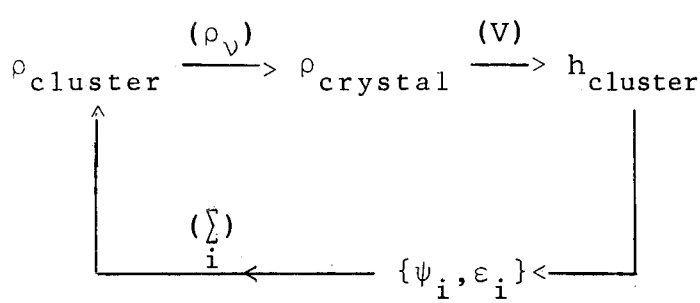

shows the essential features of decomposition of cluster density into component ions, summation to form crystal density and potentials, solution of the SCF equations, and orbital density summation to provide input for further cycles[24,25]. In the case of ionic solids Ewald summation[26] is used to accelerate convergence of the Coulomb potential.

The self-consistent scheme just described would produce a periodic potential in a crystalline solid, essentially identical to that used in band structure calculations. Indeed, the resulting charge densities, spectral densities, and cohesive energies are in rather good agreement when one takes into account the small cluster size (2-3 shells of neighbors) typically employed. However, there is a difficulty, which surfaces when ones uses sufficiently flexible basis sets: the exterior atom/ion wells generate core states which are capable of stripping electrons from the cluster. The physical reason that this does not occur is that these states are occupied and the Pauli exclusion principle generates a compensating repulsive interaction. Pseudo-potential arguments[27] can be used to truncate the exterior core regions, and simple parametrized forms are used in many applications.

A more rigorous approach to wavefunction *boundary conditions* can be obtained by the cluster Green's function theory[28]. Here one obtains a localized partial wave representation of the host Green's function, removes terms connected with cluster sites, and redetermines the cluster wavefunctions in the MS framework. The computational effort required here is heavy, with applications primarily being in the area of metallic impurities. Less sophisticated boundary conditions have been developed by different groups to approximately satisfy the physical boundary conditions desired.

For example, in the case of metals, one can simply match the cluster wavefunction at some boundary to propagating spherical waves[29,30]. For semiconductors, it is convenient to generate bond-saturating *pseudoatoms* (typically hydrogenic) to terminate the cluster and to suppress surface states[31].

As a final practical example we discuss *basis orthogonalization* techniques, which permit us to reject (project out) undesired wavefunction components in solving the single particle cluster equations. Consider expansions of the type of Eq. (7), and demand that the conditions

$$\langle \chi_j | \phi_k \rangle = 0 \qquad \begin{matrix} j=1,2,...M \\ k=1,2,...L \end{matrix} \tag{33}$$

be satisfied. For the sake of simplicity, suppose that the reference functions $\{\phi_k\}$ are mutually orthonormal, then the operator

$$P = 1 - \sum_k |\phi_k\rangle\langle\phi_k| \tag{34}$$

will "purify" the basis, in the sense that $\tilde{\chi}_j = P\chi_j$ satisfy Eq. 33. The functions $\{\phi_k\}$ can either be taken to be atomic core states (core-orthogonalization) or exterior host-atom valence states (overlap repulsion). The operation can either be carried out directly, by numerical summation to transform $\{\chi_j\} \rightarrow \{\tilde{\chi}_j\}$, or implicitly by transforming Hamiltonian and overlap matrices in Eq. (15)

B. APPLICATIONS TO CHEMISORPTION

The DV methods with numerical basis sets have been applied in studies of the electronic structure of transition metal (TM) clusters. Free particles[32], alloys and metallic impurities[33] ligated clusters[23], surfaces and chemisorption geometries[34] have been modelled in order to gain an understanding of the metal-metal and metal-ligand bonding. In this section we will take the interaction of acetylene C_2H_2 with the Ni(111) surface as an example of applications to chemically interesting chemisorption processes.

The charge density contours of $\rho(\vec{r})$ for a clean Ni(111) surface are shown in Fig. 2; core contributions are suppressed. Here a very small Ni_3 cluster, at the center of the figure, is variational and used to generate a self-consistent embedding potential for the semi-infinite solid.

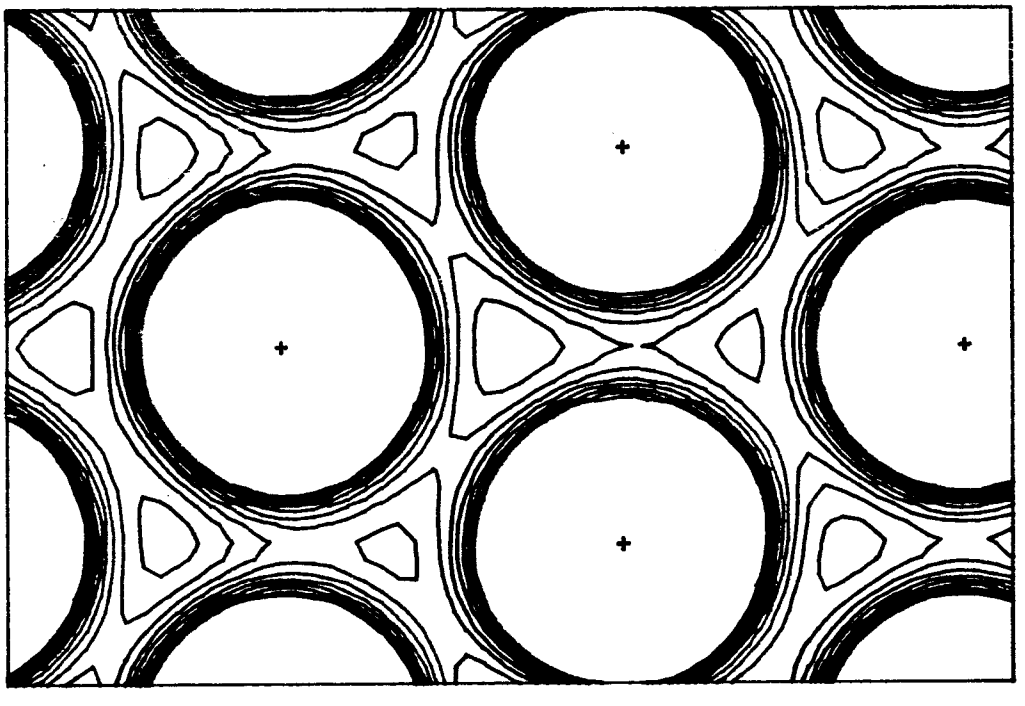

Fig. 2 - Charge density contours in Ni(111) plane; $0.03 \leq \rho \leq 0.08$ a.u. with interval 0.005 a.u. (Ref.35).

A cut perpendicular to the surface is shown in Fig. 3; the upper right-atom is variational. One can note the tendency of ρ to fill in and smooth out density variations in the surface plane, as opposed to interior regions.

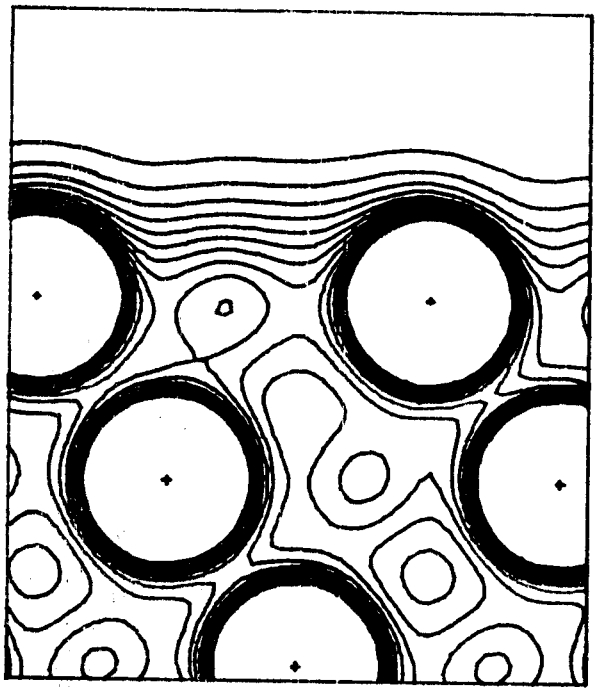

Fig. 3 - Charge density contours transverse to Ni(111) plane; intervals of 0.005 a.u. (Ref.35).

As a free molecule C_2H_2 is linear; but a variety of bonded geometries are possible on the Ni surface. Models have been proposed for plausible binding sites based upon electron diffraction (LEED), photoemission (UPS) and infrared (IR) vibrational spectra, as well as in analogy to known molecular species. The LD theory can play a useful role here in determining the relative energy and most likely conformation of metal chemisorption complexes. A long-range goal is to map sufficient portions of the interatomic poten-

tial surface to aid in construction of classical and semiclassical models of surface-reaction dynamics. Calculations were first performed on isolated C_2H_2 to calibrate the basis set and verify that good accuracy is obtained for binding energy and geometry. One of the so-called "close-coupled" sites was chosen for the present C_2H_2:Ni(111) study, with the C_2H_2 in planar geometry parallel to the surface, and the C-C axis in a bridging geometry with respect to Ni. Two parameters were varied; height of the molecular plane above the surface and C-C-H angle. Charge density in the transverse plane (Fig.4) shows the C-C bond cross-section for the minimum energy configuration. The molecular plane (Fig.5) shows a longitudinal cross-section of the C-C bond and the optimal C-C-H angle of 165^0. Further studies need to be made, particularly with the molecular plane perpendicular to the surface, and for different adsorption sites, in order to model dissociation and recombination processes.

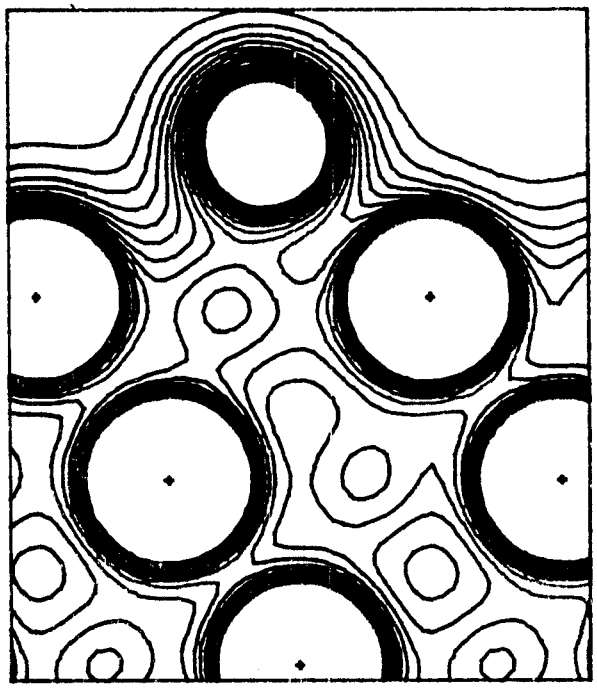

Fig. 4 - Charge density contours for C_2H_2:Ni(111) transverse to (111) plane; intervals of 0.005 a.u. (Ref.35).

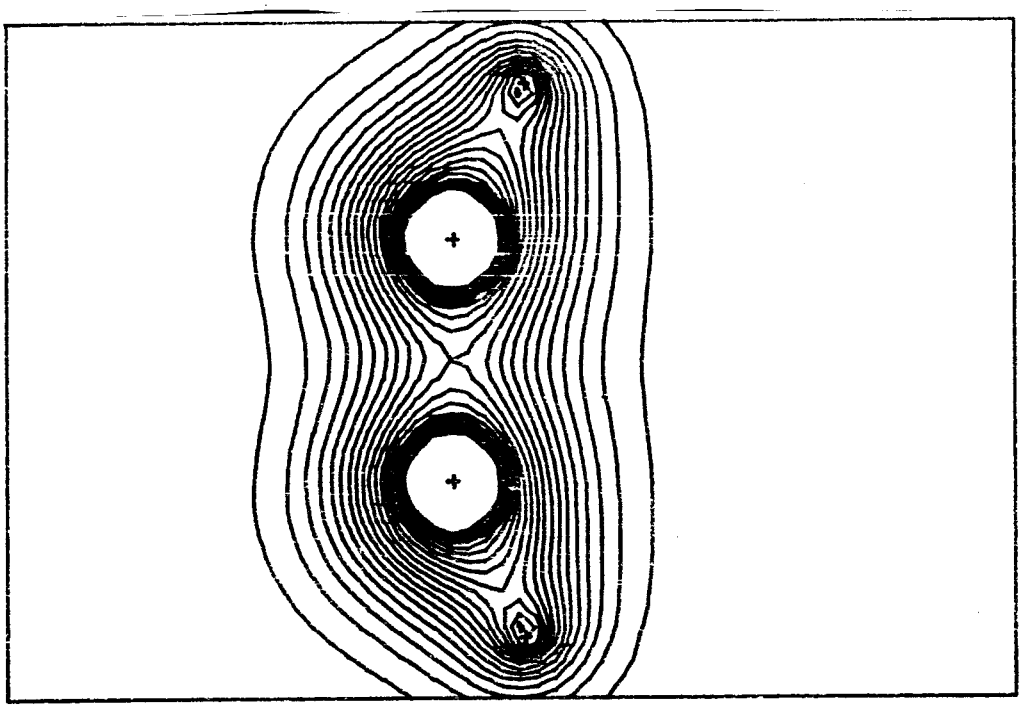

Fig. 5 - Charge density contours in C_2H_2 plane over Ni(111); intervals of 0.02 a.u.

6. RELATIVISTIC EFFECTS

We have emphasized the flexibility of DV numerical methods in treating different basis sets and incorporating various interactions in the Hamiltonian. Relativistic effects on electronic structure become important for the description of *chemical* properties for atoms of the 4d series and beyond; *inner shell properties* are affected over the entire periodic table. The Dirac equation provides an adequate single particle approach, with an effective Hamiltonian[36]

$$h_\mu = c \underset{\approx}{\alpha}.\vec{p} + \underset{\approx}{\beta} m_o c^2 + V_\mu(\vec{r}) \tag{35}$$

which can be directly utilized in the LD-SCF scheme. Here $\underset{\approx}{\alpha}$ and $\underset{\approx}{\beta}$ are the 4x4 velocity and rest-mass matrices, $c = 137.037$ (speed of light in a.u.) and V_μ is the effective potential. Fortunately, relativity does not alter the structure of the potential greatly[37,38] so that most effects can be identified with modifications in the kinetic part of h-namely, spin-orbit splitting and mass-velocity increase in binding. *Indirect effects*, which arise as self-consistent shielding alter both energy and radial wavefunctions, are of great importance in understanding relative shifts of s-, p-, and d-level structure of heavy atoms, and concomitant changes in chemical properties.

In our particular approach to the Dirac equation, four-component solutions of the atomic problem are used as basis functions[39],

$$\chi_{n\ell jm} = \begin{bmatrix} f_{n\ell_j}(r)\, Y_{\ell jm}(\hat{r},\xi) \\ g_{n\bar{\ell}_j}(r)\, Y_{\bar{\ell}jm}(\hat{r},\xi) \end{bmatrix} \tag{36}$$

where f and g are the large-and small-component radial functions respectively, and Y are spherical spinor harmonics corresponding to total angular momentum j and orbital components ℓ and $\bar{\ell}$. Magnetic effects in open-shell systems are included through a *moment-polarized* potential V_μ analogous to the *spin-polarized* potential of non-relativistic theory. Here the Kramers pairs, which are degenerate under time reversal in absence of a magnetic field, are split into two classes $\mu = \uparrow, \downarrow$.

As a simple example of relativistic effects as determined in LD theory, we display in Table 2 valence and shallow core eigenvalues for the d^8s^2 configuration of Pt.

level	relativistic	level	nonrelativistic
4s 1/2	695.6	4s	578.5
4p 1/2	587.4	4p	485.6
3/2	496.4		
4d 3/2	318.8	4d	314.7
5/2	302.0		
4f 5/2	74.6	4f	86.3
7/2	71.1		
5s 1/2	103.8	5s	83.1
5p 1/2	69.0	5p	53.9
3/2	53.8		
5d 3/2	8.2	5d	9.4
5/2	6.8		
	0.9eV		4.8eV
6s 1/2	5.9	6s	4.6
6p 1/2	1.1	6p	0.9
3/2	0.5		
E_{tot} (x10^5)	5.0192786		4.7169316

Table 2 - Orbital and total energies (eV) for d^8s^2 platinum atom ($\alpha = 0.7$, spin restricted) in NR and DS models.

7. APPLICATIONS TO CERAMIC OXIDES

Ceramic oxide materials provide a severe challenge to electronic structure theories, due to their complex and varied composition. Their properties are typically very dependent upon intrinsic defect structure, and sensitive to (deliberate or accidential) impurity doping. Technical and industrial applications are very wide-ranging, including structural materials, recording and microwave device components, catalysts and sensors, nonlinear electronic circuit elements, and the new class of high-temperature superconductors, among others. It would require too much space to reproduce here the material presented at this School. This section will consist of an extended Abstract, and the reader is invited to consult the literature for further details.

Using the DV-LD scheme with an embedded cluster model of the extended solid, we have considered TM monoxides with the rock-salt structure. In the early TM series, compounds like T_iO_x and VO_x ($x \neq 1$ denotes deviations from stoichiometry) exhibit numerous vacancies on both metal and oxygen sublattices, with properties ranging from metallic to semiconducting. Diffuse X-ray scattering studies and K-shell absorption cross-sections have been used to characterize the vacancy structures and to probe local relaxation phenomena[40,41]. Toward the middle of the 3d series compounds like wustite $Fe_{1-x}O$ form interstitial defect complexes associated with $M^{2+} \rightarrow M^{3+}$ valence changes. Aggregates of the 4:1 tetrahedral (4 metal vacancies, 1 interstitial metal) complex are considered to dominate electronic and thermodynamic properties. These materials, including MnO and CoO may be termed magnetic semiconductors or insulators, with antiferromagnetic ordering commonly observed. Cohesive energy calculations

based on small (8 atom) or moderate sized (27 atom) clusters allow the determination of energy of various defect arrangements relative to the unperturbed lattice. The 4:1 interstitial with Fe^{3+} at the center is in fact found to be the most stable isolated defect in $Fe_{1-x}O$, confirming interpretations of Mössbauer, X-ray, and neutron scattering data[42]. Aggregates of this complex formed by edge - or vertex-sharing (7:2 <110> and 7:2 <111>) are also found to be energetically favored, and are thus expected to be present in high concentration at elevated temperatures. In CoO the 4:1 complex also appears to be most stable; however, the simple metal vacancy lies close in energy. Thus 1:0 defects can be present in significant numbers and contribute to diffusion and conduction processes[43]. Experiments in progress will help to distinguish between different processes present in Mn, Fe and Co monoxide, and check our prediction that in MnO the 4:1 interstitial is relatively unfavored.

Zirconia, ZrO_2, provides an example of a structural ceramic, whose native defect state consists of oxygen vacancies. The addition of divalent ions such as Ca^{2+} or trivalent ions such as y^{3+} as substituents on the Zr^{4+} sites stabilizes the cubic phase. Cluster calculations have shown that $O^{=}$ vacancies reduce the intrinsic band gap from $\sim$6.5 eV to $\sim$5 eV, also introducing "impurity levels" in the mid-gap region. Divalent metal counterions reduce the gap to $\sim$2 eV, with impurity states appearing near the top of the valence band. Trivalent impurities produce a band gap of $\sim$3.2 eV, with mid-gap impurity levels.

Neutron diffraction studies have shown that certain oxygen near neighbors move off of lattice sites, to partially compensate for the "hole" made by a vacancy. Charge density difference maps $\Delta\rho = \rho$ (reference) $- \rho$ (defect-crystal) clearly show the ionic na-

ture of bonding in ZrO_2 and reveal the polarization of electron density induced by defects and their counterions[44]. Work in progress is aimed toward relating $\Delta\rho$ and the associated energy changes ΔE with observed changes in bulk dielectric constant.

The superconducting copper-oxide ceramics form as variants of the *perovskite* structure. The first-discovered high T_c material of this class $La_{2-x}(Sr,Ba)_xCuO_4$, with $T_c \sim 35K$, is actually a semiconductor in the "pure" phase, and one of the principal questions has been: Does doping ($Ba^{2+} \rightarrow La^{3+}$) merely stabilize the geometrical structure required for superconductivity, or do accompanying electronic charge compensations such as $Cu^{2+} \rightarrow Cu^{3+}$ provide the essential difference? X-ray absorption near edge structure (XANES) measurements and cross-section calculations of Cu K-edge processes suggest that Cu^{3+} is present in significant concentration even in the undoped material, and that the ratio $2^+:3^+$ changes very little upon doping[45].

Self consistent cluster calculations on CuO_6La_8, CuO_6La_7Ba and related embedded complexes show that the Cu-O bond is highly covalent. The Cu near-neighbor environment is distorted octahedral, with four short (equatorial) and two long (axial) bonds. In a larger perspective there exist sheets of square-planar Cu-O arrays, coupled to the rest of the lattice through the axial bonds. We find that the critical electronic levels of the unperturbed lattice consist of *occupied* $d(x^2-y^2)$-O planar and *vacant* $d(3z^2-r^2)$-O axial states, separated by only 0.03 eV. The occupied level, of 86%d character, corresponds roughly to the Cu^{2+} configuration, while the empty level, of 57%d character, could be termed a "valence excitation". Small changes in Cu-O relative bond lengths, such as are produced by lattice vibrations, or perturbations on lattice sites, including sub-

stitution of neighboring La by Ba, are sufficient to invert the level ordering thus driving the valence excitation. These results and literally thousands of other investigations now under way point toward new mechanisms of superconducting pair formation and stabilization.

The materials with highest confirmed $T_c \sim 90K$, such as $yBa_2Cu_3O_{7-x}$ present further challenges for construction of a viable theory. There are *two* types of copper; one in four-fold co-ordination to oxygen, forming chains (or *ribbons*) through the lattice, and the other in five-fold pyramidal co-ordination to oxygen, forming *sheets* enclosing the y^{3+} and Ba^{2+} sites. Here the chemical average valence is $\sim Cu^{+2.2}$, and one of the main unresolved questions is: Do both Cu sites contribute to superconductivity, or only the 4-fold? Since substitution of Y by magnetic rare-earth ions produces little change in T_c (in contrast to normal metal-based superconductors) the latter case seems likely.

The compositions with high T_c are characterized by an oxygen vacancy structure which is ordered, and tends to segregate the Cu-O ribbons and sheets. One is then faced with the possibility (or need!) of constructing 1D and 2D superconductivity models. Experiments on single crystals which measure anisotropy of critical fields, and of normal transport and spectroscopic properties will provide much-needed classification of what is presently a very active and confused area of research. Cluster and band-structure calculations are useful in providing a *static* picture of level structures and potential interactions, which can be incorporated in phenomenological models of the electron-pairing through lattice phonous or local modes three-body Cu-O-Cu resonances, or more exotic dynamical mechanisms[46].

ACKNOWLEDGEMENTS

DEE thanks Centro Brasileiro de Pesquisas Físicas and Laboratório Nacional de Computação Científica for use of their facilities. This work was supported in part by the U.S. Dept. of Energy, Grant No. DE-FGØ2-84ER45097.

REFERENCES

1. C.C.J. Roothaan, Revs. Modern Phys. 32, 179 (1960).

2. D.E. Ellis, Intl. J. Quantum Chem. 2S, 35 (1968).

3. D.E. Ellis and G.S. Painter, Phys. Rev. B2, 2887 (1970).

4. E.J. Baerends, D.E. Ellis and P. Ros, Chem. Phys. 2, 41 (1973).

5. J.C. Slater, *The Self-Consistent Field for Molecules and Solids.* (McGraw-Hill, New York) 1974.

6. H.F. Schaefer III., ed., *Applications of Electronic Structure Theory* (Plenum, New York, 1977).

7. I. Lindgren and J. Morrison, *Atomic Many-Body Theory* (Springer-Verlag, Berlin, 1982).

8. H. Goldstein, *Classical Mechanics* (Addison-Wesley. Reading. Mass) 1950.

9. K.H. Johnson, J. Chem. Phys. 45, 3085 (1966).

10. C.M. Bender and S.A. Orszag, *Advanced Math. Meth. for Scientists and Engineers* (McGraw-Hill, New York, 1978).

11. P. Tong and J.N. Rossettos, *Finite Element Method* (MIT Press, Cambridge, Mass.) 1977.

12. C.B. Haselgrove, Math. Computation 15, 323 (1961).

13. R.A. Friesner, Chem. Phys. Lett. 116, 39 (1985); J. Chem. Phys. 85, 1462 (1986).

14. A.H. Stroud, *Approximate Calculation of Multiple Integrals,* (Prentice-Hall, Englewood Cliffs, NJ, 1971).

15. D.E. Ellis, D. Guenzburger and H.B. Jansen, Phys. Rev. B 28, 3697 (1983).

16. P.M. Boerrigter, E.J. Baerends and J.G. Snijders, to be published.

17. A.C. Pedroza, this volume.

18. O.K. Andersen, Phys. Rev. B 12, 3060 (1975).

19. A. Rosén, D.E. Ellis, H. Adachi and F.W. Averill, J. Chem. Phys. 65, 3629 (1976).

20. B. Delley and D.E. Ellis, J. Chem. Phys. 76, 1949 (1982).

21. J. Guo and D.E. Ellis, to be published.

22. J.D.M. Vianna, this volume.

23. G.F. Holland, D.E. Ellis and W.C. Troger, J. Am. Chem. Soc. 108, 1884 (1986); G.F. Holland, D.E. Ellis, D.R. Tyler, H.B. Gray and W.C. Trogler, J. Am. Chem. Soc. 109, 4276 (1987).

24. M. Press and D.E. Ellis, Phys. Rev. B 35, 4438 (1987).

25. D.E. Ellis, G.A. Benesh and E. Byrom, Phys. Rev. B 16, 3308 (1977); *ibid* B 20, 1198 (1979).

26. M.P. Tosi, *Solid State Physics*, eds. F. Seitz and D. Turnbull, (Academic, NY, 1964) Vol. 16, p. 1.

27. W.A. Harrison, *Pseudopotentials in the Theory of Metals* (Benjamin, New York) 1966.

28. P.J. Braspenning, R. Zeller, A. Loder and P.H. Dederichs, Phys. Rev. B 29, 703 (1984) and references therein.

29. V.I. Anisimov, V.A. Gubanov, D.E. Ellis and E.Z. Kurmaev, J. Phys. F 11, 405 (1981).

30. B. Lindgren and D.E. Ellis, Phys. Rev. B 26, 636 (1982).

31. A.Fazzio, J.R. Leite and M.L. DeSiqueira, J. Phys. C 12, 513 (1979).

32. G.F. Holland, D.E. Ellis and W.C. Trogler, J. Chem. Phys. 83, 3507 (1985).

33. D. Guenzburger and D.E. Ellis, Phys. Rev. B 31, 93 (1985); D.E. Ellis and D. Guenzburger, Phys. Rev. B 31, 1514 (1985); D. Guenzburger, D.E. Ellis and J. Danon, J. Mag. Magn. Matls. 59, 139 (1986).

34. S.H. Chou, F.W. Kutzler, D.E. Ellis and P.L. Cao, Surf. Sci. 164, 85 (1985).

35. D.E. Ellis, J. Guo and H.P. Cheng, to be published.

36. H.A. Bethe and R.W. Jackson, *Intermediate Quantum Mechanics* (McGraw-Hill, New York) 1968.

37. D.E. Ellis, J. Phys. B 10, 1 (1977).

38. A.H. MacDonald and S.H. Vosko, J. Phys. C 12, 2977 (1979).

39. A. Rosén and D.E. Ellis, J. Chem. Phys. 62, 3039 (1975).

40. M. Morinaga and J.B. Cohen, Acta Crystallogr. Sect. A32, 387 (1976); 35,745 (1979); 35, 975 (1979).

41. F.W. Kutzler and D.E. Ellis, Phys. Rev. B 29, 6890 (1984).

42. S.H. Chou, J. Guo and D.E. Ellis, Phys. Rev. B 34, 12 (1986); M. Press and D.E. Ellis, Phys. Rev. B 35, 4438 (1987).

43. P.K. Khowash and D.E. Ellis, Phys. Rev. B, to be published.

44. D.E. Ellis, Phys. Chem. Minerals 14, 303 (1987); W.Y. Ching, D.E. Ellis and D.J. Lam, to be published.

45. E.E. Alp, G.K. Shenoy, D.G. Hinks, D.W. Capone, L. Soderholm, H.B. Schuttler, J. Guo, D.E. Ellis, P.A. Montano, and M. Ramanathan, Phys. Rev. B 35, 7199 (1987).

46. N. Mott, Nature 327, 185 (1987); P.W. Anderson and E. Abrahams, Nature 327, 363 (1987).